Supplementary data and figures

Table S1 Crystallographic data for the four compounds [a]

Compound	Eu-OA-DSTP	Tb-OA-DSTP	Eu-BDC-DSTP	Tb-BDC-DSTP
Formula	$EuC_{22}H_{13}N_3O_8S_2$	$TbC_{22}H_{13}N_3O_8S_2$	$EuC_{25}H_{19}N_3O_{10}S_2$	$EuC_{25}H_{19}N_3O_{10}S_2$
Formula weight	633.43	670.39	737.51	744.47
Crystal color	yellow	yellow	yellow	yellow
Dimensions/mm^3	0.240×0.050×0.025	0.135×0.027×0.021	0.088×0.037×0.010	0.144×0.092×0.040
Crystal system	monoclinic	monoclinic	triclinic	triclinic
Space group	C2/c	C2/c	$P\bar{1}$	$P\bar{1}$
a/Å	20.080(6)	19.929(7)	10.826(4)	10.803(3)
b/Å	18.657(5)	18.593(6)	12.044(4)	12.027(3)
c/Å	13.864(4)	13.833(5)	12.046(4)	12.040(3)
α/^{0}	90	90	109.677(3)	109.6780(10)
β/^{0}	117.570(4)	117.925(4)	103.108(2)	103.133(3)
γ/^{0}	90	90	109.545(2)	109.48
V/Å^3	4604(2)	4529(3)	1287.7(7)	1283.1
Z	8	8	2	2
D_{calcd} /g cm^{-3}	1.914	1.967	1.902	1.927
F(000)	2600	2616	730	734
μ/mm^{-1}	2.962	3.364	2.663	2.985
θ for data collection/^{0}	2.19 to 27.51	2.19 to 27.51	2.01 to 27.47	2.01 to 27.48
Reflections collected	5094	5097	5571	5444
Unique reflections/R(int)	4258/0.0524	4491/0.0563	5053/0.0426	4976/0.0421
Parameters	352	325	371	371
GOF	1.027	1.044	1.067	1.036
$R1$, $wR2$ ($I > 2\sigma(I)$)	0.0535, 0.1395	0.0591, 0.1440	0.0359, 0.1069	0.0339, 0.1029
$R1$, $wR2$ (all data)	0.0644, 0.1471	0.0698, 0.1585	0.0442, 0.1543	0.0441, 0.1623

[a] $R1 = \sum(|F_o| - |F_c|)/\sum|F_o|$, $wR2 = [\sum w(F_o^2 - F_c^2)^2/\sum w(F_o^2)^2]^{0.5}$

Table S2 The molar ratio of Tb_xEu_{1-x}-OA-DSTP and Tb_xEu_{1-x}-BDC-DSTP calculated by Inductively coupled plasma (ICP) analysis.

Sample	The molar ratio of the starting Tb/Eu salt	The Tb/Eu ratio calculated by ICP analysis
$Tb_{0.99}Eu_{0.01}$-OA-DSTP	0.99:0.01	0.9873:0.0125
$Tb_{0.99}Eu_{0.01}$-BDC-DSTP	0.99:0.01	0.9915:0.0096
$Tb_{0.98}Eu_{0.02}$-OA-DSTP	0.98:0.02	0.9792:0.0193
$Tb_{0.98}Eu_{0.02}$-BDC-DSTP	0.98:0.02	0.9814:0.0208

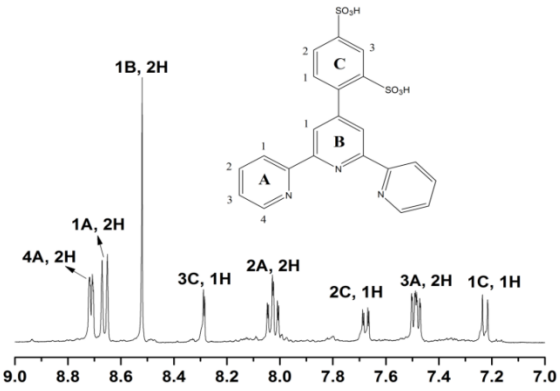

Fig. S1 ^{1}H NMR (DMSO) of 2,4-(2,2':6',2"-terpyridin-4'-yl)-benzenedisulfonic acid.

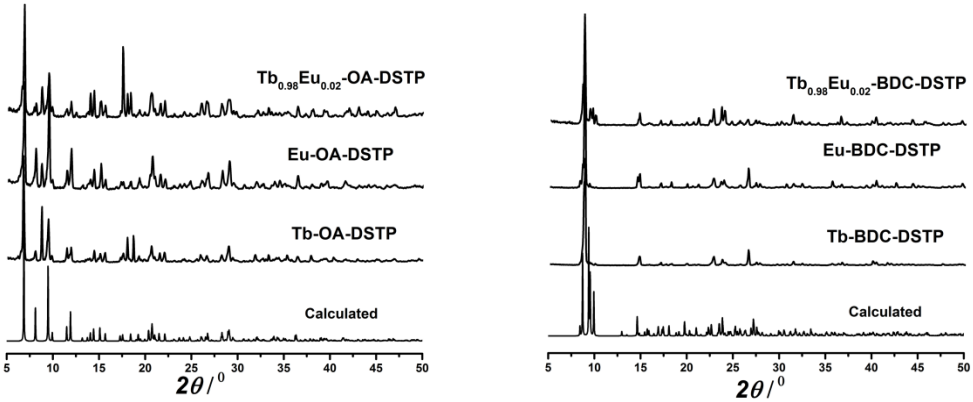

Fig. S2 Powder X-ray diffraction (PXRD) patterns.

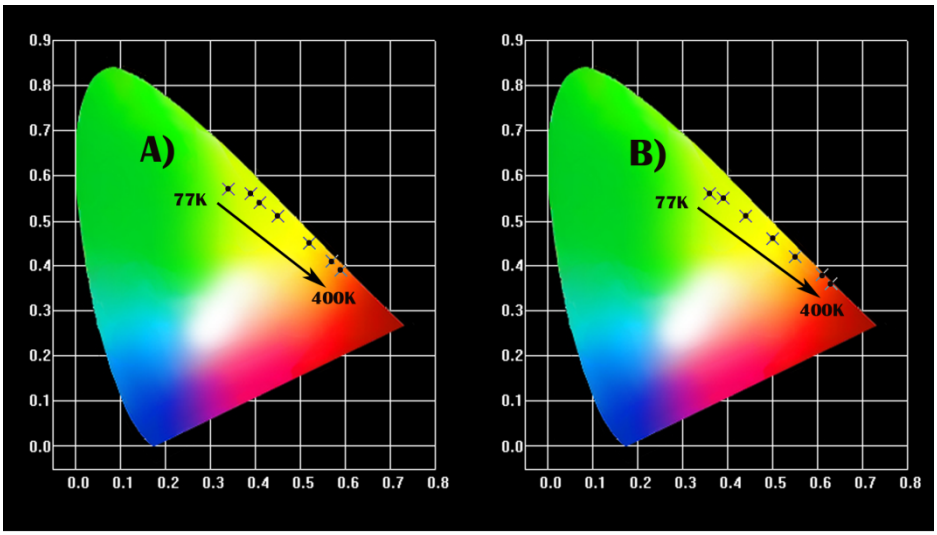

Fig. S3 The Commission International d'Eclairage (CIE) chromaticity diagram showing the luminescence color of $Tb_{0.98}Eu_{0.02}$-OA-DSTP (a) and $Tb_{0.98}Eu_{0.02}$-BDC-DSTP (b) at different temperature.

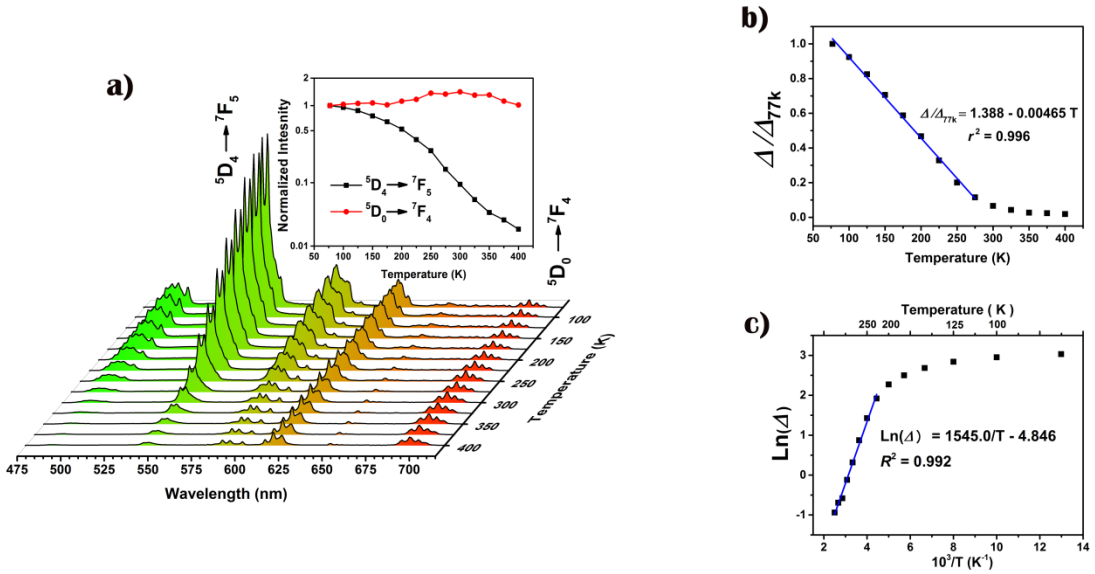

Fig. S4 The ratiometric temperature-sensing properties of $Tb_{0.99}Eu_{0.01}$-OA-DSTP: (a) emission spectra for the solid sample recorded between 77 and 400K upon excitation at 360nm, inset: normalized emission intensities of $^5D_4 \rightarrow {}^7F_5$ transition of Tb^{3+} (546nm) and $^5D_0 \rightarrow {}^7F_4$ transition of Eu^{3+} (696nm); (b) temperature-dependent intensity ratio (Δ/Δ_{77k}) and linearly fitted curve; (c) the natural logarithm of the thermometric parameter Δ changing with the inverse of temperature and the linearly fitted curve.

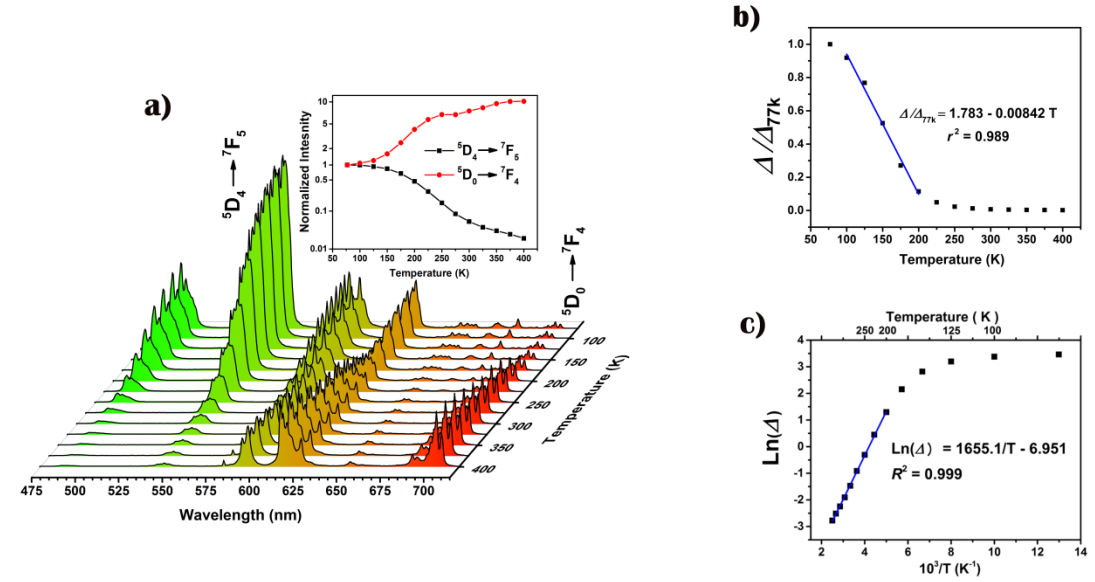

Fig. S5 The ratiometric temperature-sensing properties of $Tb_{0.99}Eu_{0.01}$-BDC-DSTP: (a) emission spectra for the solid sample recorded between 77 and 400K upon excitation at 360nm, inset: normalized emission intensities of $^5D_4 \rightarrow {}^7F_5$ transition of Tb^{3+} (546nm) and $^5D_0 \rightarrow {}^7F_4$ transition of Eu^{3+} (702nm); (b) temperature-dependent intensity ratio (Δ/Δ_{77k}) and linearly fitted curve; (c) the natural logarithm of the thermometric parameter Δ changing with the inverse of temperature and the linearly fitted curve.

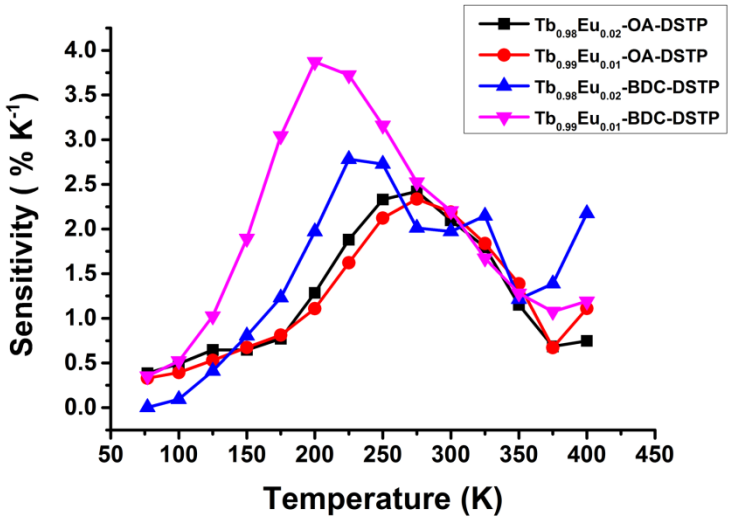

Fig. S6 Relative sensitivity of the thermometers $Tb_{1-x}Eu_x$-OA-DSTP and $Tb_{1-x}Eu_x$-BDC-DSTP (x = 0.01, 0.02).

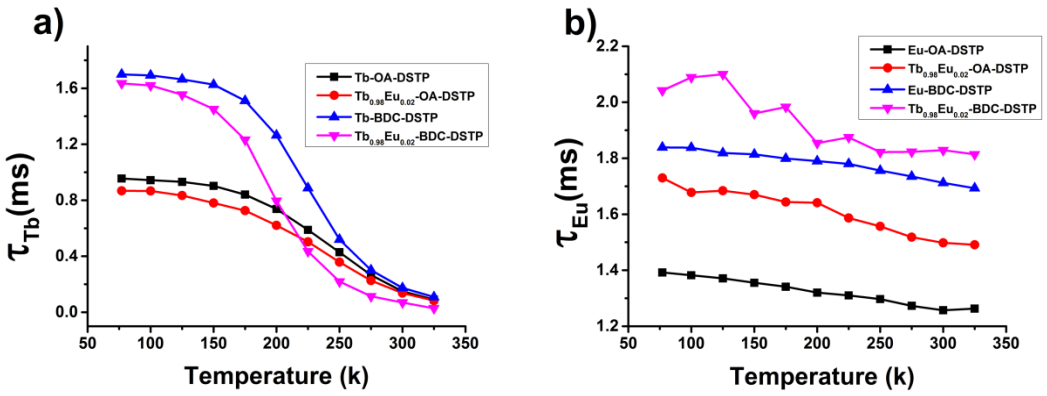

Fig. S7 The comparison of lifetimes of Tb^{3+} (a) and Eu^{3+} (b) in the pure MOFs and Tb/Eu-codoping MOFs.

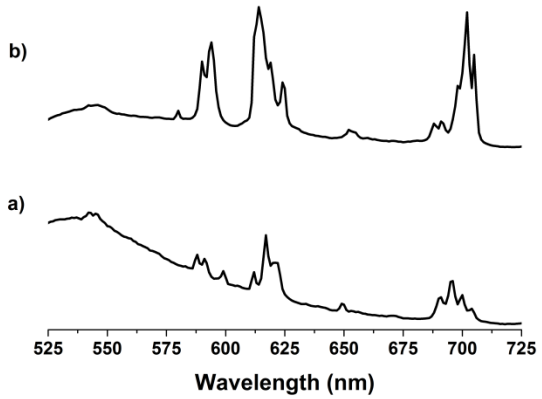

Fig. S8 The emission spectra of $Tb_{0.98}Eu_{0.02}$-OA-DSTP (a) and $Tb_{0.98}Eu_{0.02}$-BDC-DSTP (b) upon excitation of 488nm at room temperature.

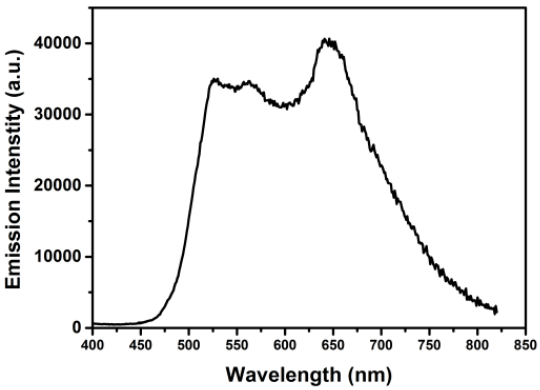

Fig. S9 Phosphorescence spectrum of Gd-OA-DSTP in the solid state at 77K.